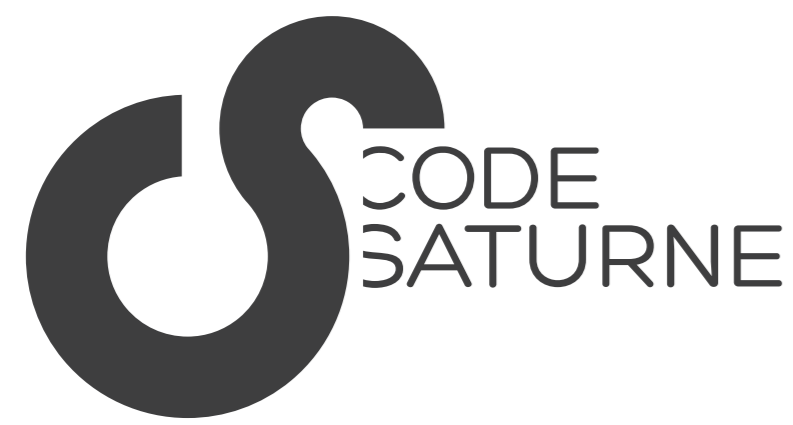


Numerical investigations on cavitation intensity for 3D homogeneous unsteady viscous flows



C. Leclercq^{a,b}, M. Vandelle^a, A. Archer^a,
R. Fortes-Patella^b, O. Hurisse^a & E. Poyart^a

^aEDF R&D, Chatou, France. ^bLEGI, Grenoble, France.

christophe.leclercq@edf.fr



High flow velocities cause regions of low pressure where vapour structures are generated. These cavitating structures collapse rapidly after reaching a region of higher pressure and are able to cause performance loss, vibration and can damage the material.

The main problem of simulating cavitation erosion is the fact that it deals with several length and time scales phenomena and involves both fluid and mechanical behavior.

The cavitation intensity - or cavitation aggressiveness - represents the mechanical loading imposed by the cavitating flow to the material. Erosion, defined as mass loss, can then be deduced from this quantity using methods as in [3] and [4]. The present work objective is to define such a flow quantity from posttreatments of 3D flow simulations.

Code Saturne with cavitation module main features

The cavitation module of *Code Saturne* is a homogeneous approach resolving the Navier-Stokes incompressible equations with void fraction (α) transport equation ([2] for more details).

$$\begin{cases} \frac{\partial \alpha}{\partial t} + \text{div}(\alpha \mathbf{u}) = \frac{\Gamma_v}{\rho_v}, \\ \frac{\partial \rho}{\partial t} + \text{div}(\rho \mathbf{u}) = 0, \\ \frac{\partial \rho \mathbf{u}}{\partial t} + \text{div}(\mathbf{u} \otimes \rho \mathbf{u}) = -\nabla p + \text{div}(\boldsymbol{\tau}). \end{cases}$$

with $\rho = \alpha \rho_v + (1 - \alpha) \rho_l$ the density ($\rho_v = 1 \text{ kg.m}^{-3}$ and $\rho_l = 1000 \text{ kg.m}^{-3}$) and Γ_v the vapourisation source term. This source term is modeled using the Merkle model [6], $\Gamma_v(\alpha, p) = m^+ + m^-$, with :

$$m^+ = -\frac{C_{prod} \rho_l \min(p - p_{sat}, 0) (1 - \alpha)}{\frac{1}{2} \rho_l u_{\infty}^2 t_{\infty}} \quad \text{and} \quad m^- = -\frac{C_{dest} \rho_v \max(p - p_{sat}, 0) \alpha}{\frac{1}{2} \rho_l u_{\infty}^2 t_{\infty}}.$$

Here $C_{prod} = 10.000$, $C_{dest} = 50$, $t_{\infty} = l_{\infty}/u_{\infty}$ ($l_{\infty} = 0.1 \text{ cm}$, $u_{\infty} = 15 \text{ to } 30 \text{ m.s}^{-1}$), and $p_{sat} = 2000 \text{ Pa}$.

A standard $k-\epsilon$ turbulent model with Reboud correction [1] is used. The resolution scheme is based on a co-located fractional step scheme, which is associated with the SIMPLEC-type algorithm.

Sub-mesh modelisation - Energy approach

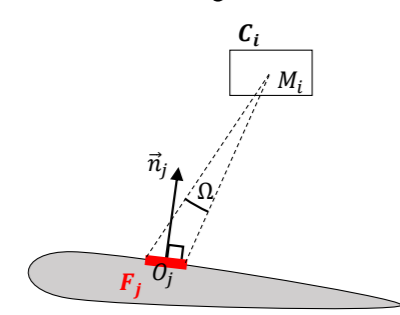
Based on the idea of Pereira [7], we can calculate a cavitation energy (E_{cav}) for each cell :

$$E_{cav} = (p - p_{sat}) \alpha V_{cell} \quad \text{expressed in } J \quad (\text{with } V_{cell} \text{ the cell volume}).$$

Then, we can deduce the cavitation power (\mathcal{P}_{cav}) of those structures for each cell and separate it in two parts (see equation (1)). The first one takes into account the contribution of the void fraction derivative, and the second one deals with the pressure derivative influence.

$$\frac{\mathcal{P}_{cav}}{V_{cell}} = -\frac{1}{V_{cell}} \frac{dE_{cav}}{dt} = \frac{\mathcal{P}_{\alpha}}{V_{cell}} + \frac{\mathcal{P}_p}{V_{cell}} \quad [W.m^{-3}], \quad \text{with} \quad \begin{cases} \frac{\mathcal{P}_{\alpha}}{V_{cell}} = -\frac{(p - p_{sat})}{\rho_l - \rho_v} \text{div}(\mathbf{u}), \\ \frac{\mathcal{P}_p}{V_{cell}} = -\alpha \left(\frac{\partial p}{\partial t} + \mathbf{u} \cdot \text{grad}(p) \right). \end{cases} \quad (1)$$

By using the solid angle (Ω) [8], we can deduce the cavitation power applied on the material surface (\mathcal{P}^{mat} , see Figure 1 and equation (2)), which defines the quantity we will name the **instantaneous cavitation intensity**.



$$\frac{\mathcal{P}^{mat}_j}{\Delta S_j} = \frac{1}{\Delta S_j} \sum_i \frac{\Omega_{ij}}{4\pi} \mathcal{P}_{cavi} \quad [W.m^{-2}]. \quad (2)$$

Figure 1: Projection of the volumic potential power on the wall.

Application to a cavitating flow around a hydrofoil

General description

Our prediction model has been applied to a NACA 65012 hydrofoil (chord length is 100mm and span 150mm) tested in the cavitation tunnel of the LMH-EPFL [7] (see Figure 2).

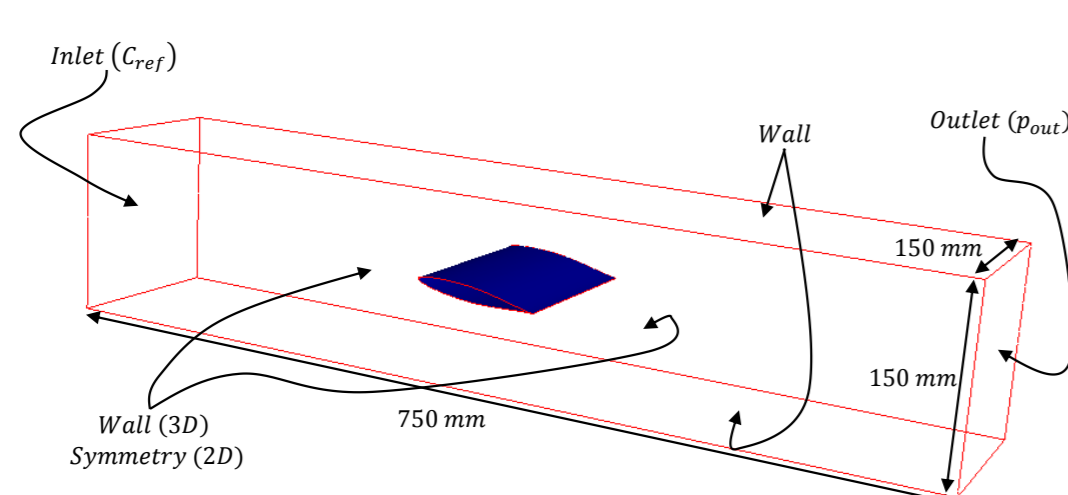


Figure 2: Description of the cavitation tunnel and computational domain with boundary conditions.

i	C_{ref}	σ [-]		
[°]	[m.s ⁻¹]	2D	3D	Exp
6°	15	1.37	1.41	1.59
	20	1.38	1.41	1.60
	25	1.41	1.44	1.62
	30	1.40	1.43	1.63

Table 1: 2D, 3D simulated and experimental [7] conditions on inlet σ ($l/L = 40\%$).

Experimental conditions tested by Pereira [7] and simulated are summarized in the Table 1. C_{ref} describes the mean axial flow velocity at the inlet of the tunnel, i the attack angle of the hydrofoil, σ the inlet cavitation number (see equation (3)), l the cavitation sheet length and L the hydrofoil chord.

$$\sigma = \frac{p_{in} - p_{sat}}{0.5 \rho_l C_{ref}^2}, \quad (3)$$

Hydrodynamic results

In order to validate the cavitating flow behaviour, we will first calibrate the cavitation sheet length (by iteration on the outlet pressure, see Figure 3) and then compare the cavitating structures shedding frequency of the experimental results with the simulated one (see Figure 4). Figure 5 illustrates the computational C-grid applied in the present study.

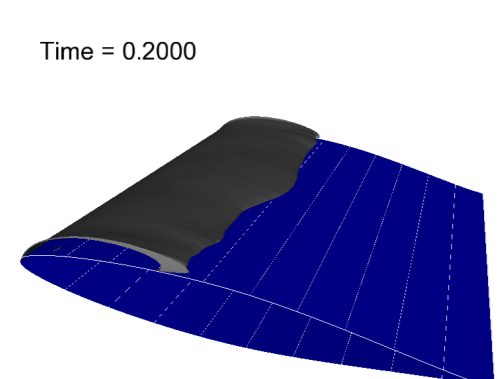


Figure 3: Iso-surface at 10% of the void fraction on the NACA65012 - $C_{ref} = 15 \text{ m.s}^{-1}$.

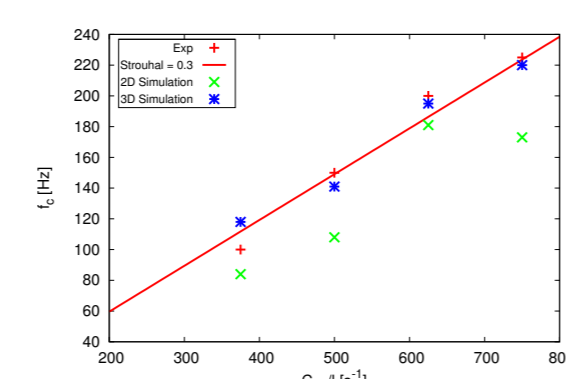


Figure 4: Shedding frequency function of reduced frequency for experimental (with linear regression at $S_r = 0.3$) [7], 2D and 3D simulations results.

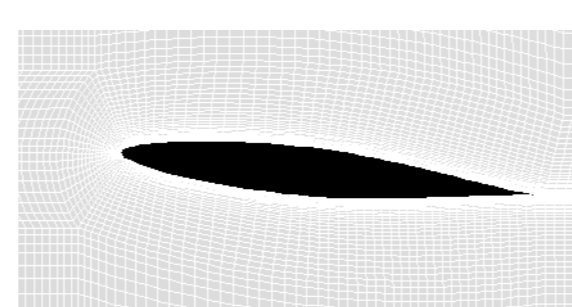


Figure 5: Mesh close to the hydrofoil.

2D and 3D simulations based on the same boundary conditions have different shedding frequencies. Even if the cavitating sheet length are the same ($l/L = 40\%$) the 3D dynamic is quite faster than the 2D one. One notes that we do not have exactly the same inlet cavitation number (σ) for 2-D and 3-D cases.

Cavitation intensity results

We first calculate the cavitation power in the fluid. Then we evaluate the cavitation intensity on the hydrofoil surface (see Figure 6).

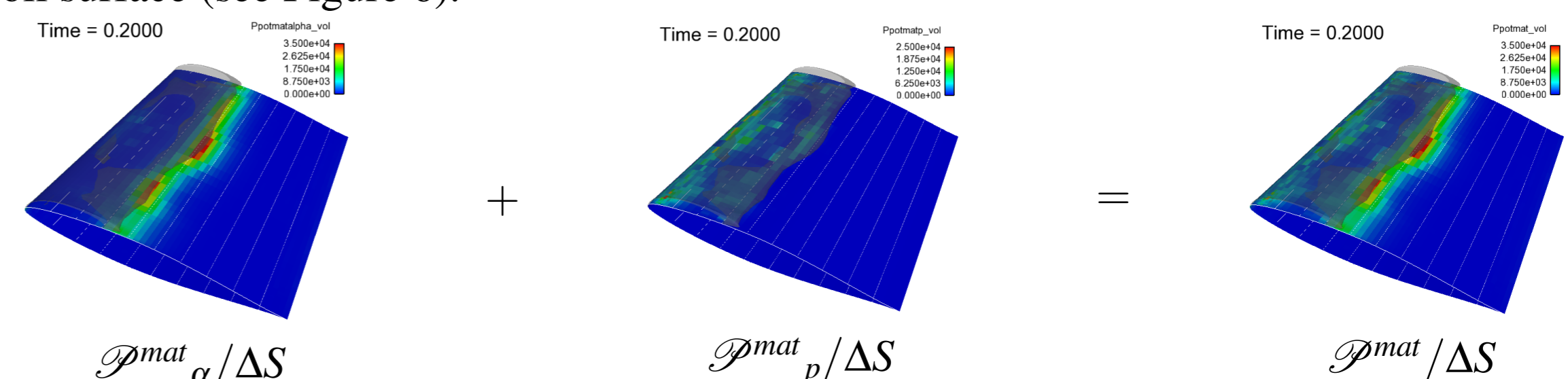


Figure 6: Visualisation of the surface instantaneous surface power on the foil - $C_{ref} = 15 \text{ m.s}^{-1}$.

We can finally add up all the received surface power ($\mathcal{P}^{mean}/\Delta S$) by each surface and divide the result by the number of time steps (N) to have a mean loading (see equation 4), which can be used as a qualitative representation of the eroded region.

$$\frac{\mathcal{P}^{mean}}{\Delta S} = \frac{1}{N} \sum_{i=1}^N \frac{\mathcal{P}^{mat}_i}{\Delta S}, \quad (4)$$

Cavitation intensity analysis

We compare our results with the experimental volume damage rate given by pitting tests (V_d i.e. the deformed volume divided by the analyzed sample surface area and test duration) [3]. By taking cavitation sheet length of 50% ($\sigma = 1.34$), 3D simulation matches much better with experimental results (see Figure 7).

Quantitatively, 3-D simulations are a bit more erosive for the hydrofoil because of the transverse elements contribution (3-D effect) (see Figure 8).

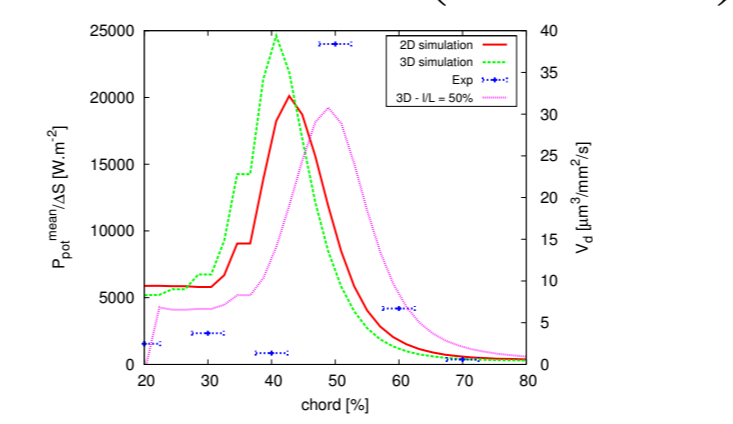


Figure 7: Cavitation intensity and experimental results according to the foil chord - $C_{ref} = 15 \text{ m.s}^{-1}$.

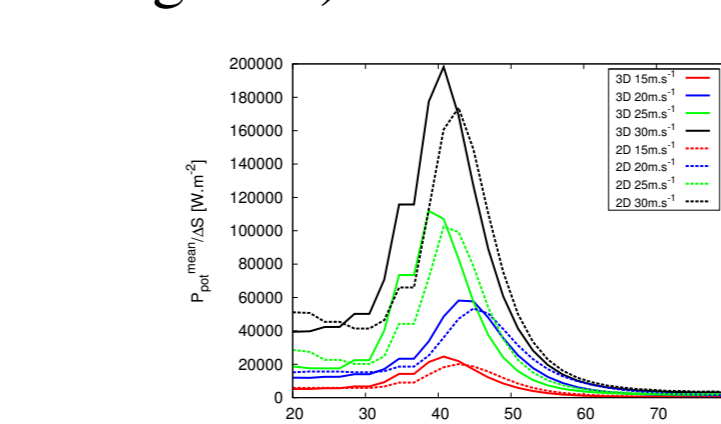


Figure 8: $\mathcal{P}^{mean}/\Delta S$ along the chord for different velocities

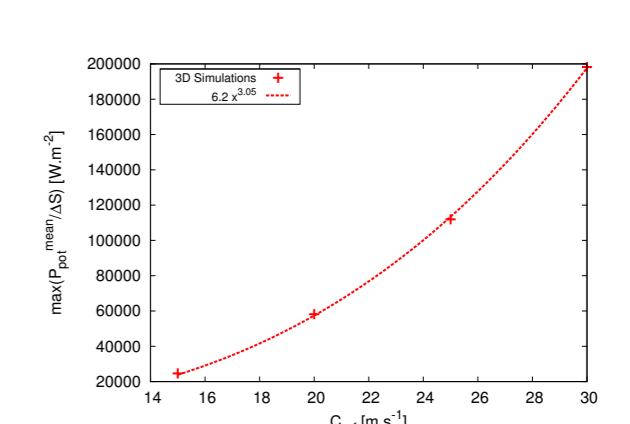


Figure 9: Maximum $\mathcal{P}^{mean}/\Delta S$ value as a function of C_{ref} .

Figure 9 shows the relation between the maximum cavitation intensity value and the inlet velocity. We find $\mathcal{P}^{mean}/\Delta S = 6.2 C_{ref}^3$ for the 3D case, which agrees with the literature.

Perspectives

Bubble scale simulations

A local model is in progress to better understand the phenomena at bubble scale and to improve our sub-mesh model using a compressible homogeneous prototype of *Code Saturne* [5].

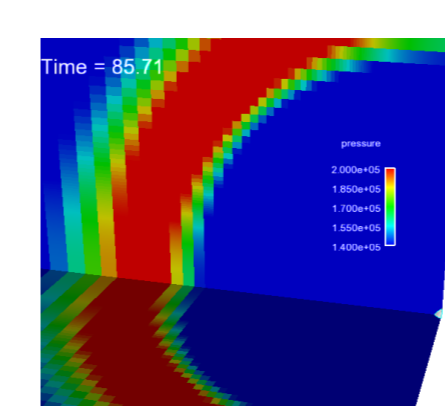


Figure 10: Simulation of a bubble implosion in an infinite volume (Pressure on the wall and rebound of the bubble, time in μs).

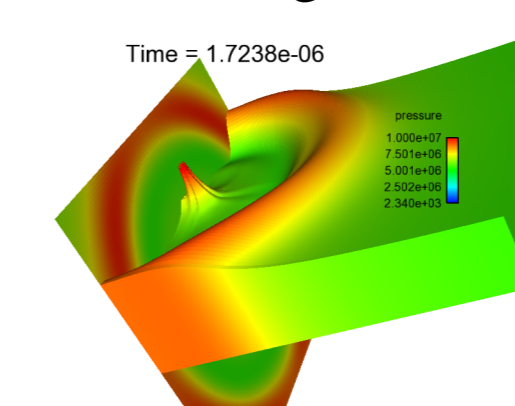


Figure 11: Simulation of a bubble implosion near a wall (Pressure on the wall and rebound of the bubble, time in s).

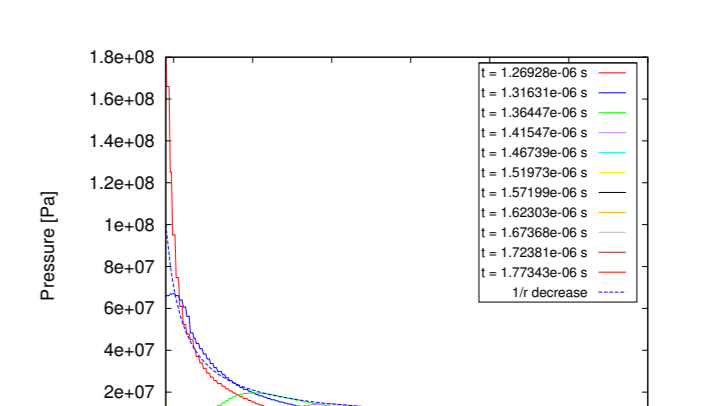


Figure 12: Radial distribution of the pressure applied to a solid wall ($\gamma = L/R = 1.4$).

Pump simulations

Simulation of the erosion intensity in centrifugal pumps is one of the major applications of the present model. In order to prepare this future work, the ability of *Code Saturne* to simulate cavitating flows in centrifugal pump is analyzed on the full geometry of the SHF pump (see Figure 13 and 14).

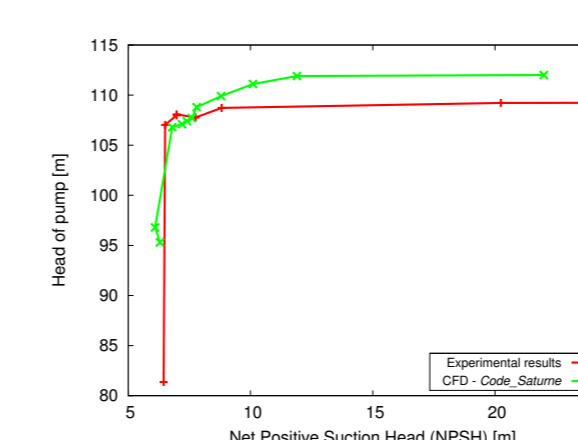


Figure 13: Cavitation effect on SHF pump performances, comparison with experimental.

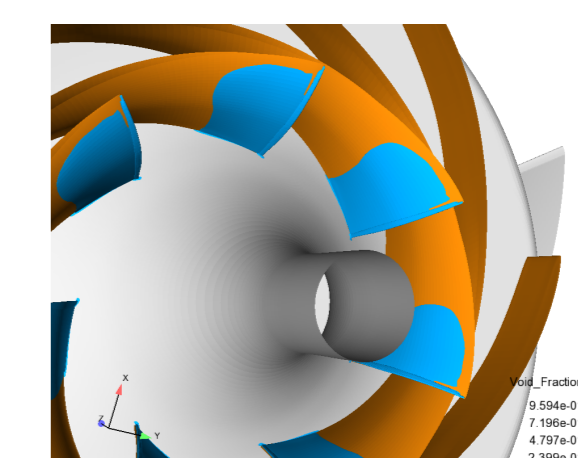


Figure 14: Cavitation sheets at nominal flow rate (NPSH = 7.8 m).

A cavitation intensity model has been developed using *Code Saturne* with cavitation module. Comparisons between numerical and available experimental results allow the qualitative and quantitative validation of the proposed approach concerning the prediction of the flow unsteady behavior, of the location of erosion area and of the influence of flow velocity on the cavitation intensity. The comparative analyses of 2D and 3D numerical results indicated that 3D effects should be taken into account to obtain reliable quantitative evaluations of the potential power applied on the foil.

References

- Coutier-Delgosha, O., Fortes-Patella, R., Reboud, J.L.: Evaluation of the turbulence model influence on the numerical simulations of unsteady cavitation. *Journal of Fluids Engineering* **125**(1), 38–45 (2003)
- EDF R&D (2014). URL <http://www.code-saturne.org>
- Fortes-Patella, R., Archer, A., Flageul, C.: Numerical and experimental investigations on cavitation erosion. In: IOP Conference Series : Earth and Environmental Science, vol. 15, p. 022013. IOP Publishing (2012)
- Fortes-Patella, R., Chofat, T., Reboud, J.L., Archer, A.: Mass loss simulation in cavitation erosion: Fatigue criterion approach. *Wear* **300**(1), 205–215 (2013)
- Hurisse, O.: Application of an homogeneous model to simulate the heating of two-phase flows. *International Journal on Finite Volumes* **11**, <http://www.lap.univ-mrs.fr/IDFV/spip.php?article52> (2014)
- Li, D., Merkle, C.: A unified framework for incompressible and compressible fluid flows. *Journal of Hydrodynamics* **B**(18 (3)), 113–119 (2006)
- Pereira, F., Avelian, F., Dupont, P.: Prediction of cavitation erosion: an energy approach. *Journal of Fluids Engineering* **120**(4), 719–727 (1998)
- Van Oosterom, A., Strackee, J.: The solid angle of a plane triangle. *IEEE transactions on Biomedical Engineering* **2**(BME-30), 125–126 (1983)